

Phononic Josephson oscillation and self-trapping with two-phonon exchange interaction

Xun-Wei Xu,^{1,*} Ai-Xi Chen,^{2,1,†} and Yu-xi Liu^{3,4}

¹*Department of Applied Physics, East China Jiaotong University, Nanchang, 330013, China*

²*Department of Physics, Zhejiang Sci-Tech University, Hangzhou, 310018, China*

³*Institute of Microelectronics, Tsinghua University, Beijing 100084, China*

⁴*Tsinghua National Laboratory for Information Science and Technology (TNList), Beijing 100084, China*

(Dated: May 25, 2017)

We propose a bosonic Josephson junction (BJJ) in two nonlinear mechanical resonator coupled through two-phonon exchange interaction induced by quadratic optomechanical couplings. The nonlinear dynamic equations and effective Hamiltonian are derived to describe behaviors of the BJJ. We show that the BJJ can work in two different dynamical regimes: Josephson oscillation and macroscopic self-trapping. The system can transfer from one regime to the other one when the self-interaction and asymmetric parameters exceed their critical values. We predict that a transition from Josephson oscillation to macroscopic self-trapping can be induced by the phonon damping in the asymmetric BJJs. Our results opens up a way to demonstrate BJJ with two-phonon exchange interaction and can be applied to other systems, such as the optical and microwave systems.

I. INTRODUCTION

Bosonic Josephson junction (BJJ), a bosonic analog of the superconducting Josephson junction, was first proposed and observed in two weakly coupled Bose-Einstein condensates [1–10] to study macroscopic tunneling. After that BJJ has also been studied both theoretically and experimentally in other nonlinear bosonic systems, such as coupled nonlinear optical cavities [11–18] and nanomechanical resonators [19]. One important application of BJJ is to serve as a quantum interference device [20]. As a two-mode Bose-Hubbard model, BJJ also offers a simple platform to explore quantum many-body dynamics [21].

In contrast to all hitherto realized BJJs, where two nonlinear bosonic systems are coupled by hopping of single bosons, we here propose a BJJ in two nonlinear mechanical modes coupled through two-phonon exchange interaction. The Bose-Hubbard model with atom-pair tunneling [22–26] or two-photon exchange [27–33] has been studied for years. However, the realization of two-phonon exchange interaction in the mechanical systems is still lack of effective method.

Recently, multi-mode optomechanical system [34], that multiple mechanical resonators are coupled to a single cavity mode via radiation pressure or optical gradient forces, provides us an appropriate platform to realize nonlinear phononic interaction mediated by the cavity mode [35–39]. We find that two-phonon exchange interaction can be induced by coupling two mechanical modes to a common cavity mode through quadratic optomechanical interactions. An effective Hamiltonian for two nonlinear mechanical modes with two-phonon exchange interaction is obtained by adiabatically eliminating the cavity mode. We show that the transition between Josephson oscillation and macroscopic self-trapping (MST) can be observed by tuning the parameters blow (or above) certain critical values.

Different from the BJJs with single-boson hopping inter-

action, where four distinct modes are predicted [2–4], i.e., zero-phase mode, running-phase mode, π -phase oscillations, and π -phase self-trapping, whereas in our system, there are three distinct modes, i.e., zero-phase mode, $\pi/2$ -phase oscillations, and running-phase mode. In addition, a dynamic transition from Josephson oscillation to MST induced by phonon damping is predicted for asymmetric BJJ with two-phonon exchange interaction, which is very different from the previous theoretical predictions [4, 16] and experimental observations [12].

The paper is organized as follows. In Sec. II, we derive an effective Hamiltonian for two nonlinear mechanical modes coupled through two-phonon exchange interaction from a multi-mode quadratic optomechanical system with two nonlinear mechanical modes and one cavity mode. In Sec. III, an effective Hamiltonian for BJJ are obtained from the two nonlinear mechanical modes coupled through two-phonon exchange interaction. The behavior of the BJJ in the non-self-interacting and linear regimes is discussed in Sec. IV. In Sec. V, we study the dynamic behaviors for the symmetric BJJ. The effective potential for BJJ is shown in Sec. VI. We study the effect of the phonon damping on the dynamic behavior of the asymmetric BJJ in Sec. VII. Finally, we summarize results in Sec. VIII.

II. TWO-PHONON EXCHANGE INTERACTION

As schematically shown in Fig. 1, we study a system that two nonlinear mechanical modes are coupled to a common cavity mode with quadratic optomechanical couplings. Such system can be realized by either two partly reflective nonlinear membranes in a Fabry-Perot cavity [40], optomechanical crystal [41–43], or other systems. The Hamiltonian of these systems can be written as

$$H = \sum_{i=1,2} \left[\omega_i^{(0)} b_i^\dagger b_i + U_i^{(0)} b_i^\dagger b_i^\dagger b_i b_i + g_i a^\dagger (b_i^\dagger + b_i)^2 \right] + \omega_c a^\dagger a + (\Omega a^\dagger e^{-i\omega a t} + \text{H.c.}), \quad (1)$$

*Electronic address: davidxu0816@163.com

†Electronic address: aixichen@ecjtu.edu.cn

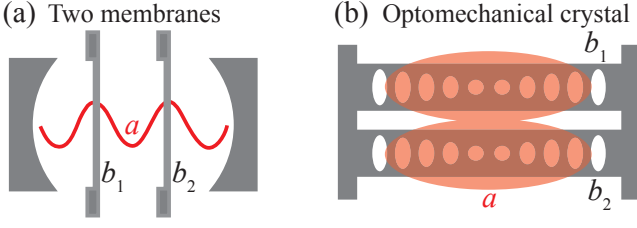


FIG. 1: (Color online) Schematic diagram of two nonlinear mechanical modes (b_1 and b_2) coupled to a common cavity mode (a) through quadratic optomechanical interactions: (a) two partly reflective nonlinear membranes in a Fabry-Perot cavity; (b) optomechanical crystal.

where a and a^\dagger are the annihilation and creation operators of the cavity mode with frequency ω_c , b_i and b_i^\dagger ($i = 1, 2$) are the annihilation and creation operators of the i th nonlinear mechanical mode with frequency $\omega_i^{(0)}$ and nonlinearity strength $U_i^{(0)}$, and g_i is the quadratic optomechanical coupling strength between the cavity mode and the i th mechanical mode. The cavity mode is driven by an external field with the strength Ω and frequency ω_d .

The dynamics of the mechanical oscillators and cavity mode can be described by quantum Langevin equations. After considering the dissipations and within the mean-field approximation, we can obtain the dynamical equations

$$\frac{d}{dt}b_i = -\left(\frac{\gamma_i}{2} + i\omega_i^{(0)}\right)b_i - i2U_i^{(0)}b_i^\dagger b_i b_i - i2g_i a^\dagger a (b_i^\dagger + b_i), \quad (2)$$

$$\frac{d}{dt}a = -\left\{\frac{\kappa}{2} + i\left[\Delta_c + \sum_{i=1,2} g_i (b_i^\dagger + b_i)^2\right]\right\}a - i\Omega, \quad (3)$$

for $i = 1, 2$, with the damping rates of the cavity mode κ and mechanical modes γ_i ($i = 1, 2$). Here, $\Delta_c \equiv \omega_c - \omega_d$ is the detuning between the cavity mode and driving field. To solve the above nonlinear dynamical equations, we can write each operator as the sum of its steady-state value and the time-dependent term: $a \rightarrow \alpha + \tilde{a}$ and $b_i \rightarrow \beta_i + \tilde{b}_i$, where α and β_i are the steady-state values of the system. When $g_i \geq 0$, the steady-state values are

$$\alpha = \frac{-i2\Omega}{\kappa + i2\Delta_c}, \quad (4)$$

$$\beta_i = 0. \quad (5)$$

Under the assumption that the external driving is strong (i.e., $|\alpha| \gg 1$), $|\alpha|^2 \gg \langle a^\dagger a \rangle$, and frequency shift induced by the quadratic optomechanical couplings is small, $\Delta_c \gg \left\langle \sum_{i=1,2} g_i (b_i^\dagger + b_i)^2 \right\rangle$, the dynamical equations for the time-dependent terms are given by

$$\begin{aligned} \frac{d}{dt}\tilde{b}_i &= -\left(\frac{\gamma_i}{2} + i\omega_i\right)\tilde{b}_i - i2U_i^{(0)}\tilde{b}_i^\dagger \tilde{b}_i \tilde{b}_i - i2g_i |\alpha|^2 \tilde{b}_i^\dagger \\ &\quad - i2g_i (\alpha a^\dagger + \alpha^* a + a^\dagger a) (\tilde{b}_i^\dagger + \tilde{b}_i), \end{aligned} \quad (6)$$

$$\frac{d}{dt}\tilde{a} = -\left(\frac{\kappa}{2} + i\Delta_c\right)\tilde{a} - i\sum_{i=1,2} g_i \alpha (\tilde{b}_i^\dagger + \tilde{b}_i)^2, \quad (7)$$

where $\omega_i = \omega_i^{(0)} + 2g_i |\alpha|^2$.

After introducing the slowly varying amplitudes $\tilde{a} \equiv \alpha e^{(i\Delta_c + \kappa/2)t}$ and $\tilde{b}_i \equiv b_i e^{i\omega_i t}$, under the rotating-wave approximation (by keeping the terms with low frequencies $\Delta_i \equiv \Delta_c - 2\omega_i$ and neglecting oscillating terms with high frequencies, e.g. ω_i , Δ_c , etc) with $|\Delta_i| \ll \{\omega_i, \Delta_c\}$, we have

$$\frac{d\tilde{b}_i}{dt} = -i2U_i^{(0)}\tilde{b}_i^\dagger \tilde{b}_i \tilde{b}_i - i2G_i^* \tilde{a} \tilde{b}_i^\dagger e^{-i(\Delta_i + \kappa/2)t} - \frac{\gamma_i}{2}\tilde{b}_i, \quad (8)$$

$$\frac{d\tilde{a}}{dt} = -i\sum_{i=1,2} G_i \tilde{b}_i^2 e^{(i\Delta_i + \kappa/2)t}, \quad (9)$$

where $G_i = g_i \alpha$ is the effective optomechanical coupling strength. The expression of \tilde{a} can be obtained as

$$\tilde{a} = -i\sum_{i=1,2} \int_{-\infty}^t G_i \tilde{b}_i^2 e^{(i\Delta_i + \kappa/2)\tau} d\tau. \quad (10)$$

Under the assumption that the damping rate of the cavity mode is much larger than the effective optomechanical couplings G_j and the damping rates of the mechanical modes, i.e., $\kappa \gg \{G_j, \gamma_i\}$, the evolution of \tilde{b}_i is much slower than \tilde{a} , so \tilde{b}_i can be taken out of the integrals, then we have [44, 45]

$$\tilde{a} = -i\sum_{i=1,2} \frac{2G_i}{\kappa + i2\Delta_i} \tilde{b}_i^2 e^{(i\Delta_i + \kappa/2)t}. \quad (11)$$

After adiabatically eliminating the cavity mode by substituting Eq. (11) and $b_i \equiv \tilde{b}_i e^{-i\omega_i t}$ into Eq. (8), the dynamical equations for the mechanical modes b_i become

$$\frac{db_1}{dt} = -\left(\frac{\gamma_1}{2} + i\omega_1\right)b_1 - i2U_1 b_1^\dagger b_1 b_1 + i2J_1 b_2 b_2 b_1^\dagger, \quad (12)$$

$$\frac{db_2}{dt} = -\left(\frac{\gamma_2}{2} + i\omega_2\right)b_2 - i2U_2 b_2^\dagger b_2 b_2 + i2J_2 b_1 b_1 b_2^\dagger, \quad (13)$$

where the effective nonlinearity strength $U_i = U_i^{(0)} - |G_i|^2 / (\Delta_i - i\kappa/2)$ and effective two-phonon exchange coupling strengths $J_1 = -g_1 g_2 |\alpha|^2 / (\Delta_2 - i\kappa/2)$ and $J_2 = -g_1 g_2 |\alpha|^2 / (\Delta_1 - i\kappa/2)$ can be controlled by tuning the strength Ω and frequency ω_d of the external field. We choose $\{|\Delta_1 - \Delta_2|, \kappa\} \ll |\Delta_i|$, so that $U_i \approx U_i^{(0)} - g_i^2 |\alpha|^2 / \Delta_i$ and $J \approx -g_1 g_2 |\alpha|^2 / \Delta_1 \approx -g_1 g_2 |\alpha|^2 / \Delta_2$, and a Hermitian Hamiltonian can be obtained as (without considering the damping terms)

$$H_{\text{eff}} = \sum_{i=1,2} \left(\omega_i b_i^\dagger b_i + U_i b_i^\dagger b_i^\dagger b_i b_i \right) + J \left(b_1^\dagger b_1^\dagger b_2 b_2 + b_2^\dagger b_2^\dagger b_1 b_1 \right), \quad (14)$$

which describes a model for two nonlinear mechanical modes coupled through two-phonon exchange interaction.

III. BOSONIC JOSEPHSON JUNCTION

From Eq. (14), we can verify that, when the effect of mechanical damping can be neglected, the total phonon population $N_T = n_1 + n_2$ is constant, where n_i is the phonon population in the i th mechanical mode. For large phonon numbers, i.e., $N_T \gg 1$, the operators of the mechanical modes can be treated as classical quantities,

$$b_i = \sqrt{n_i} e^{i\theta_i}, \quad (15)$$

where θ_i is the phase. By introducing the population imbalance $z \equiv (n_1 - n_2)/N_T$ and the phase difference $\phi \equiv \theta_2 - \theta_1$ between the two mechanical modes, the dynamics of the mechanical modes can be rewritten as the nonlinear equations

$$\frac{dz}{dt} = (1 - z^2) \sin 2\phi, \quad (16)$$

$$\frac{d\phi}{dt} = \Delta + gz - z \cos 2\phi, \quad (17)$$

where the time has been rescaled as $2JN_T t \rightarrow t$, and the dimensionless parameters are $g = (U_1 + U_2)/2J$, $\Delta = \Delta_0 + \Delta_u$ with $\Delta_0 = (\omega_1 - \omega_2)/2JN_T$ and $\Delta_u = (U_1 - U_2)/2J$. We can see that these nonlinear dynamical equations are invariant under the transformation $\Delta \rightarrow -\Delta$, $\phi \rightarrow -\phi + \pi/2$ and $g \rightarrow -g$.

We can consider z and ϕ as two canonically conjugate variables, then an effective Hamiltonian (derived from the above equation with $dz/dt = -\partial H_J/\partial\phi$ and $d\phi/dt = \partial H_J/\partial z$) for BJJ is obtained as

$$H_J = \Delta z + \frac{g}{2} z^2 + \frac{1}{2} (1 - z^2) \cos 2\phi. \quad (18)$$

The BJJ tunneling current is defined by

$$I \equiv \frac{N_T}{2} \frac{dz}{dt} = JN_T^2 (1 - z^2) \sin 2\phi. \quad (19)$$

IV. NON-SELF-INTERACTING AND LINEAR REGIMES

Before the detailed analysis of the BJJ with numerical solutions, here we consider the behavior of the system in the non-self-interacting and linear regimes. For symmetric BJJ without self-interaction, i.e., $\Delta = g = 0$, the dynamical equation for z is obtained as

$$\frac{d^2 z}{dt^2} = -2z(1 - z^2). \quad (20)$$

This can yield a harmonic oscillation for z only in the limit $|z| \ll 1$ with frequency

$$\omega_0 = 2\sqrt{2}JN_T. \quad (21)$$

In this case the BJJ tunneling current I is an alternating current (AC) with frequency $2\sqrt{2}JN_T$.

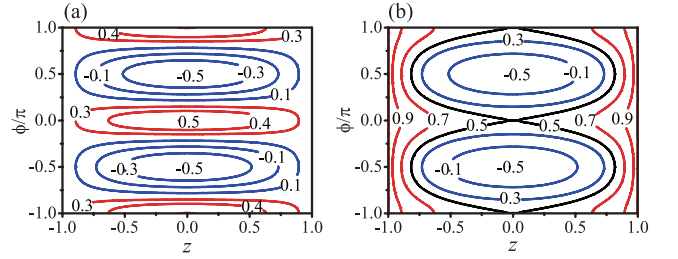


FIG. 2: (Color online) Energy contours of a symmetric bosonic Josephson junction versus z and ϕ , for (a) $g = 0.5$ and (b) $g = 2.0$.

For symmetric BJJ ($\Delta = 0$) with $g < 1$, in the linear limit ($|z| \ll 1$ and $|\phi| \ll 1$), the dynamical equation for z is given by

$$\frac{d^2 z}{dt^2} = 2(g - 1)z. \quad (22)$$

z oscillates harmonic with frequency

$$\omega_L = 2\sqrt{2(1-g)}JN_T. \quad (23)$$

Then the frequency of the AC current I become $2\sqrt{2(1-g)}JN_T$.

Still in the linear limit ($|z| \ll 1$ and $|\phi| \ll 1$) with $g < 1$, if the BJJ is asymmetric with parameter $\Delta \gg (g - \cos 2\phi)z$, then we have

$$\phi = \phi(0) + \Delta t, \quad (24)$$

$$z = z(0) - \frac{1}{2\Delta} \cos [2\phi(0) + 2\Delta t]. \quad (25)$$

z oscillates harmonically with frequency

$$\omega_{ac} = 2\Delta. \quad (26)$$

The BJJ tunneling current is given by

$$I = JN_T^2 \sin [2\phi(0) + 2\Delta t]. \quad (27)$$

An AC current I is produced in the asymmetric BJJ working in the linear limit.

V. SYMMETRIC BJJ

For a symmetric BJJ, i.e., $\Delta = 0$, the Hamiltonian in Eq. (18) becomes

$$H_J = \frac{g}{2} z^2 + \frac{1}{2} (1 - z^2) \cos 2\phi. \quad (28)$$

Figure 2 shows the energy contours of a symmetric BJJ for different values of self-interaction parameter g . We can find that the location of the energy minima, maxima, and saddle points crucially depends upon the self-interaction parameter g . For $g < 1$ (strong two-phonon exchange coupling, i.e.,

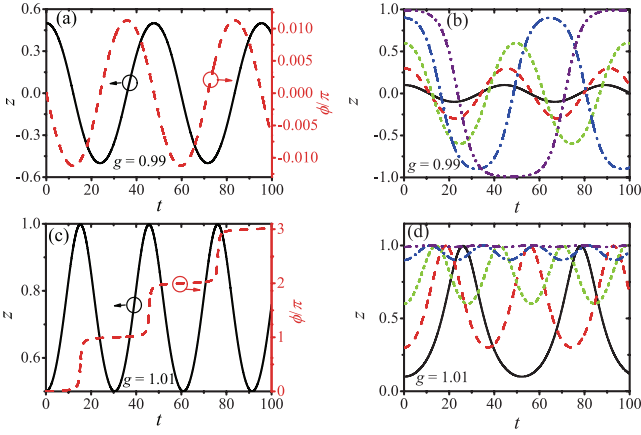


FIG. 3: (Color online) Population imbalance z and phase difference ϕ/π as functions of the rescaled time t for $g = 0.99$ in (a) and (b), $g = 1.01$ in (c) and (d). The initial imbalance in (a) and (c) is $z(0) = 0.5$. In (b) and (d), the imbalance takes the initial values 0.1 (black solid), 0.3 (red dash), 0.6 (green dot), 0.9 (blue dash-dot), 0.99 (purple dash-dot-dot). The other parameters are $\Delta = 0$ and $\phi(0) = 0$.

$U_i < J$), the minima are at $[z, \phi] = [0, (m + 1/2)\pi]$ (m is an integer) and the maxima settle in $[z, \phi] = [0, m\pi]$, whereas for $g > 1$ (strong nonlinearities, i.e. $U_i > J$), the minima are still at $[z, \phi] = [0, (m + 1/2)\pi]$, while $[z, \phi] = [0, m\pi]$ become saddle points. This transition of the point $[z, \phi] = [0, m\pi]$ from a local maximum to a saddle point is a manifestation of the transition of the Josephson oscillation regime to the self-trapping regime.

For a given value of the initial population imbalance $z(0)$, if the self-interaction parameter g exceeds a critical value g_c , the populations become macroscopically self-trapped with $\langle z \rangle \neq 0$. This corresponds to the macroscopic self-trapping (MST) condition for

$$H_0 \equiv H_J(z(0), \phi(0)) > \frac{1}{2}, \quad (29)$$

and the critical self-interaction parameter for MST is

$$g_c = \left\{ 1 - \left[1 - z(0)^2 \right] \cos[2\phi(0)] \right\} \frac{1}{z(0)^2}. \quad (30)$$

Figure 3 describes the time evolution of population imbalance z for different values of self-interaction parameter g . Figures 3(a) and 3(c) show the transition from the Josephson oscillation to the MST regime at $g = 1$, for the specific initial conditions $[z(0), \phi(0)] = [0.5, 0]$. In Fig. 3(a), where $g < 1$, z and ϕ oscillate around $[z, \phi] = [0, 0]$, which corresponding to the zero-phase mode. In Fig. 3(c), where $g > 1$, $\langle z \rangle = 0$ and ϕ increases monotonously, which corresponding to the running-phase mode. The transition behavior for $\phi(0) = 0$ at $g = 1$ is independent of the initial value of the population imbalance, as shown in Figs. 3(b) and 3(d). We can also see this clearly from Eq. (30): $g_c = 1$ for $\phi(0) = 0$, which is independent of the population imbalance.

On the other hand, from Eq. (29), when $g > 1$ remains constant and initial value $\phi(0) \neq m\pi$ (m is an integer), there

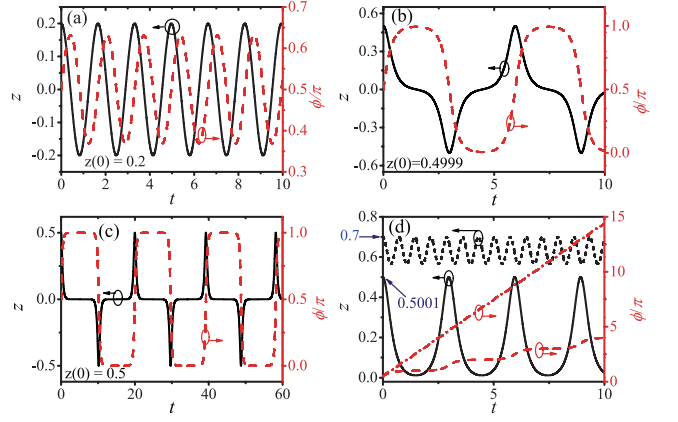


FIG. 4: (Color online) Population imbalance z and phase difference ϕ/π as functions of the rescaled time t for $\phi(0) = \pi/2$, $g = 7$ and $\Delta = 0$. The initial imbalance $z(0)$ takes the initial values (a) 0.2, (b) 0.4999, (c) 0.5, (d) 0.5001 (black solid and red dash curves) and 0.7 (black dot and red dash-dot curves).

is a critical population imbalance z_c for the initial value of the population imbalance $z(0)$ as

$$z_c = \sqrt{\frac{1 - \cos[2\phi(0)]}{g - \cos[2\phi(0)]}}. \quad (31)$$

Figure 4 shows the transition from the Josephson oscillation to the MST regime at $z(0) = z_c = 0.5$, for the specific initial conditions $[\phi(0), g] = [\pi/2, 7]$. For $z(0) < 0.5$, an increase of $z(0)$ adds higher harmonics to the sinusoidal oscillations, and the period of such oscillations increases with $z(0)$, as shown in Figs. 4(a)-(c). Meanwhile, ϕ oscillates around the point $\phi = \pi/2$, which corresponding to the $\pi/2$ -phase oscillations. MST occurs when $z(0) > z_c$ as shown in Fig. 4(d). Moreover, for $z(0) > 0.5$, the period and the amplitude of the MST oscillations decrease with $z(0)$, i.e., z becomes more localized with high oscillation frequency for larger values of $z(0)$.

VI. POTENTIAL FOR BJJ

In this section, we employ the alternative approach of examining the effective potential for the BJJ. One can use the energy H_J of Eq. (28) to describe the system in terms of an equation of motion for a classical particle moving in a potential $W(z) \equiv H_J - (dz/dt)^2$ [3] with coordinate z and total energy H_J . For symmetric BJJ ($\Delta = 0$), the potential $W(z)$ is obtained as

$$W(z) = H_0 + 4H_0^2 - 1 + 2(1 - 2H_0g)z^2 + (g^2 - 1)z^4 \quad (32)$$

with the conserved energy $H_0 = H_J$. It is clear that if $H_0 > 1/2$, we will have $W(z=0) > H_0 = H_J$ and MST sets in.

Figure 5 displays the potential $W(z)$ for (a) $\phi(0) = 0$, (b) $\phi(0) = \pi/2$. For a given value of initial conditions

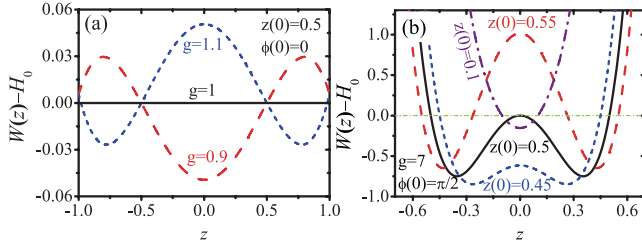


FIG. 5: (Color online) The potential $W(z) - H_0$ is plotted as a function of z for initial phase difference $\phi(0) = 0$ in (a) and $\phi(0) = \pi/2$ in (b) with $\Delta = 0$. In (a) g takes the values 0.9 (red dash), 1.0 (black solid) and 1.1 (blue dot) with the initial population imbalance $z(0) = 0.5$. In (b) initial population imbalance $z(0)$ takes the values 0.1 (purple dash-dot), 0.55 (red dash), 0.5 (black solid) and 0.45 (blue dot) with $g = 7$.

$[z(0), \phi(0)] = [0.5, 0]$, in Fig. 5(a), the the increase of the the value g , $W(z)$ is changed from a single (red dash curve) to a double (blue dot curve) well and the changeover occurs at the critical point $g = 1$ (black solid horizontal line). It is worth noting that the potential is flat at the critical point $g = 1$ corresponding to steady state for the population imbalance z . For a given value of $[\phi(0), g] = [\pi/2, 7]$, in Fig. 5(b), with the increase of $z(0)$, $W(z)$ is changed from a parabolic (purple dash-dot curve) to a double well and the changeover occurs at the point $z(0) = \sqrt{1/g}$. As the parameter g increases, the oscillations become anharmonic and the system is in the Josephson regime [also see Fig. 4(b) and 4(c)]. For $z(0) > 0.5$ the total energy is smaller than the potential barrier (red dash curve), forcing the particle to become localized in one of the two wells.

If the BJJ is asymmetric with $\Delta \neq 0$, then the potential $W(z)$ is given by

$$W(z) = H_0 + 4H_0^2 - 1 - 8H_0\Delta z + 2(1 + 2\Delta^2 - 2H_0g)z^2 + 4\Delta g z^3 + (g^2 - 1)z^4. \quad (33)$$

The potential is asymmetric because there are two terms with odd powers of z in $W(z)$. We plot $W(z) - H_0$ for different Δ in Figs. 6(a) and (b). The corresponding dynamical evolution of z is shown in Figs. 6(c) and (d). For $\Delta = 0$ the potential $W(z) - H_0$ is symmetric and z oscillates around $\langle z \rangle = 0$ for $g < g_c$. When Δ is increased, asymmetric energy is added to the potential, corresponding to $\langle z \rangle \neq 0$. If the asymmetric parameter Δ exceeds a critical value Δ_c [green dot curves, $\Delta_c = 0.05$ in Figs. 6(a) and (c), $\Delta_c \approx 0.24$ in Figs. 6(b) and (d)], the system moves into the MST regime.

VII. DAMPING INDUCED TRANSITION

We now consider the effect of the phonon damping on the dynamic behavior of the asymmetric BJJ. For simplicity, we assume that the two nonlinear mechanical modes have the same damping rates, i.e., $\gamma_0 \equiv \gamma_1 = \gamma_2$. The dynamical

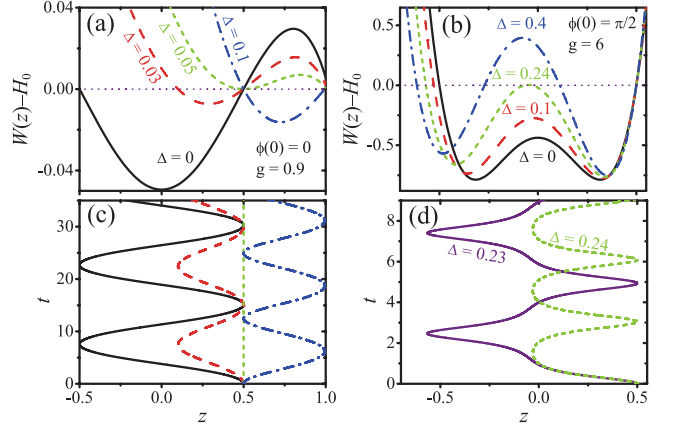


FIG. 6: (Color online) z potential $W(z) - H_0$ plotted against z for $[\phi(0) = 0, g = 0.9]$ in (a) and $[\phi(0) = \pi/2, g = 6]$ in (b) with $z(0) = 0.5$ and Δ taking different values. z is plotted as a function of the rescaled time t for $[\phi(0) = 0, g = 0.9]$ in (c) and $[\phi(0) = \pi/2, g = 6]$ in (d) with $z(0) = 0.5$ and Δ taking different values.

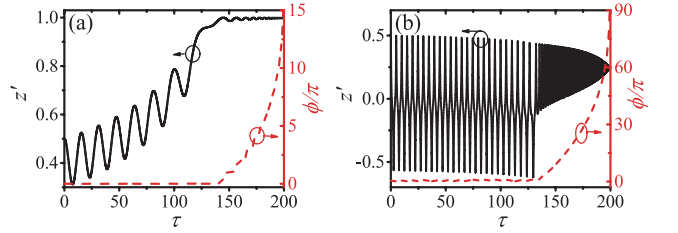


FIG. 7: (Color online) Population imbalance z' and phase difference ϕ as functions of the rescaled time τ for $\gamma = 0.01$, in (a) with $z'(0) = 0.5, \phi(0) = 0, g = 0.9, \Delta_0 = 0.03, \Delta_u = 0.01$, and in (b) with $z'(0) = 0.5, \phi(0) = \pi/2, g = 6, \Delta_0 = 0.22, \Delta_u = 0.01$.

equations in the presence of phonon damping are given by

$$\frac{dz}{dt} = (e^{-\gamma t} - z^2) \sin 2\phi - \frac{1}{2}\gamma z, \quad (34)$$

$$\frac{d\phi}{dt} = \Delta_0 + \Delta_u e^{-\frac{\gamma}{2}t} + gz - z \cos 2\phi, \quad (35)$$

where $\gamma = \gamma_0/(JN_T)$ is the dimensionless damping parameter, and N_T is the total phonon population at the initial time. The damping parameter γ is inversely proportional to the initial total phonon population N_T . In order to suppress the effect of the phonon damping, one effective way is to enhance the total phonon population N_T in the initial time.

Equations (34) and (35) can be rewritten as the dynamical equations of the effective population imbalance $z' \equiv ze^{\frac{\gamma}{2}t}$ and ϕ as

$$\frac{dz'}{d\tau} = (1 - z'^2) \sin 2\phi, \quad (36)$$

$$\frac{d\phi}{d\tau} = \frac{2\Delta_0}{2 - \gamma\tau} + \Delta_u + gz' - z' \cos 2\phi, \quad (37)$$

where the rescaled time τ is defined by $\tau \equiv \frac{2}{\gamma}(1 - e^{-\frac{\gamma}{2}t})$ for $t \in [0, +\infty)$ and $\tau \in [0, 2/\gamma)$. Equations (36) and (37) are the same as Eqs. (16) and (17) but with Δ_0 replaced by $2\Delta_0/(2 - \gamma\tau)$. This means that the asymmetric of the system are enhanced as time goes on. When the asymmetric parameter $\Delta' = 2\Delta_0/(2 - \gamma\tau) + \Delta_u$ exceeds the critical value Δ_c , the system has a transition from the Josephson oscillation into the MST. Figure 7 shows the time evolution of z' and ϕ as functions of the rescaled time τ in the presence of phonon damping, i.e., $\gamma = 0.01$. It shows that the system works in the Josephson oscillation regime at the beginning with $\Delta_0 + \Delta_u < \Delta_c$, and then moves into the MST regime when $\tau > [2 - 2\Delta_0/(\Delta_c - \Delta_u)]/\gamma$.

VIII. CONCLUSIONS

In summary, we have proposed a BJJ in two nonlinear mechanical resonator coupled through two-phonon exchange interaction. Two dynamic regimes of Josephson oscillation and MST are predicted, and the system can transfer from one regime to the other one when the self-interaction and asymmetric parameters exceed their critical values. A transition, from Josephson oscillation to MST induced by the phonon

damping, can be observed in the asymmetric BJJs. The measurement of the dynamic behaviors of the mechanical resonators could be realized by transferring the mechanical signals into electric signals through piezoelectric effect [46, 47], or into optical signals through auxiliary optomechanical couplings [19, 45, 48–50]. Our results open a way to investigate interferometer and Bose-Hubbard model with two-phonon exchange interactions in optomechanical systems. Similarly, BJJ based on two-boson exchange interaction can also be realized in the optical and microwave systems [27–33].

Acknowledgement

X.-W.X. is supported by the National Natural Science Foundation of China (NSFC) under Grants No.11604096 and the Startup Foundation for Doctors of East China Jiaotong University under Grant No. 26541059. A.-X.C. is supported by NSFC under Grants No. 11365009. Y.-X.L. is supported by the National Basic Research Program of China(973 Program) under Grant No. 2014CB921401, the Tsinghua University Initiative Scientific Research Program, and the Tsinghua National Laboratory for Information Science and Technology (TNList) Cross-discipline Foundation.

-
- [1] G. J. Milburn, J. Corney, E. M. Wright, and D. F. Walls, Quantum dynamics of an atomic Bose-Einstein condensate in a double-well potential, *Phys. Rev. A* **55**, 4318 (1997).
 - [2] A. Smerzi, S. Fantoni, S. Giovanazzi, and S. R. Shenoy, Quantum Coherent Atomic Tunneling between Two Trapped Bose-Einstein Condensates, *Phys. Rev. Lett.* **79**, 4950 (1997).
 - [3] S. Raghavan, A. Smerzi, S. Fantoni, and S. R. Shenoy, Coherent oscillations between two weakly coupled Bose-Einstein condensates: Josephson effects, π oscillations, and macroscopic quantum self-trapping, *Phys. Rev. A* **59**, 620 (1999).
 - [4] I. Marino, S. Raghavan, S. Fantoni, S. R. Shenoy, and A. Smerzi, Bose-condensate tunneling dynamics: Momentum-shortened pendulum with damping, *Phys. Rev. A* **60**, 487 (1999).
 - [5] S. Giovanazzi, A. Smerzi, and S. Fantoni, Josephson Effects in Dilute Bose-Einstein Condensates, *Phys. Rev. Lett.* **84**, 4521 (2000).
 - [6] D. Sarchi, I. Carusotto, M. Wouters, and V. Savona, Coherent dynamics and parametric instabilities of microcavity polaritons in double-well systems, *Phys. Rev. B* **77**, 125324 (2008).
 - [7] S. Backhaus, S. Pereverzev, R. W. Simmonds, A. Loshak, J. C. Davis, and R. E. Packard, Discovery of a metastable π -state in a superfluid ^3He weak link, *Nature (London)* **392**, 687 (1998).
 - [8] M. Albiez, R. Gati, J. Fölling, S. Hunsmann, M. Cristiani, and M. K. Oberthaler, Direct Observation of Tunneling and Nonlinear Self-Trapping in a Single Bosonic Josephson Junction, *Phys. Rev. Lett.* **95**, 010402 (2005).
 - [9] S. Levy, E. Lahoud, I. Shomroni, and J. Steinhauer, The a.c. and d.c. Josephson effects in a Bose-Einstein condensate, *Nature (London)* **449**, 579 (2007).
 - [10] A. Trenkwalder, G. Spagnolli, G. Semeghini, S. Coop, M. Landini, P. Castilho, L. Pezzè, G. Modugno, M. Inguscio, A. Smerzi, and M. Fattori, Quantum phase transitions with parity-symmetry breaking and hysteresis, *Nature Phys.* **12**, 826 (2016).
 - [11] K. G. Lagoudakis, B. Pietka, M. Wouters, R. André, and B. Deveaud-Plédran, Coherent Oscillations in an Exciton-Polariton Josephson Junction, *Phys. Rev. Lett.* **105**, 120403 (2010).
 - [12] M. Abbarchi, A. Amo, V. G. Sala, D. D. Solnyshkov, H. Flayac, L. Ferrier, I. Sagnes, E. Galopin, A. Lemaître, G. Malpuech, and J. Bloch, Macroscopic quantum self-trapping and Josephson oscillations of exciton polaritons, *Nature Phys.* **9**, 275 (2013).
 - [13] A. C. Ji, Q. Sun, X. C. Xie, and W. M. Liu, Josephson Effect for Photons in Two Weakly Linked Microcavities, *Phys. Rev. Lett.* **102**, 023602 (2009).
 - [14] N. Didier, S. Pugnetti, Y. M. Blanter, and R. Fazio, Detecting phonon blockade with photons, *Phys. Rev. B* **84**, 054503 (2011).
 - [15] N. S. Voronova, A. A. Elistratov, and Yu. E. Lozovik, Detuning-Controlled Internal Oscillations in an Exciton-Polariton Condensate, *Phys. Rev. Lett.* **115**, 186402 (2015).
 - [16] A. Rahmani and F. P. Laussy, Polaritonic Rabi and Josephson Oscillations. *Sci. Rep.* **6**, 28930 (2016).
 - [17] J. Larson and M. Horsdal, Photonic Josephson effect, phase transitions, and chaos in optomechanical systems, *Phys. Rev. A* **84**, 021804(R) (2011).
 - [18] J. H. Teng, S. L. Wu, B. Cui, and X X Yi, Quantum optomechanics with quadratic cavity-membrane couplings, *J. Phys. B: At. Mol. Opt. Phys.* **45**, 185506 (2012).
 - [19] Sh. Barzanjeh and D. Vitali, Phonon Josephson junction with nanomechanical resonators, *Phys. Rev. A* **93**, 033846 (2016).
 - [20] D. Gerace, H. E. Türeci, A. Imamoglu, V. Giovannetti, and R. Fazio, The quantum-optical Josephson interferometer, *Nature Phys.* **5**, 281 (2009).

- [21] M. J. Hartmann, F. G. S. L. Brandão, and M. B. Plenio, Quantum many-body phenomena in coupled cavity arrays, *Laser Photon. Rev.* **2**, 527 (2008).
- [22] S. Fölling, S. Trotzky, P. Cheinet, M. Feld, R. Saers, A. Widera, T. Müller, and I. Bloch, Direct observation of second-order atom tunnelling, *Nature (London)* **448**, 1029 (2007).
- [23] S. Zöllner, H.-D. Meyer, and P. Schmelcher, Few-Boson Dynamics in Double Wells: From Single-Atom to Correlated Pair Tunneling, *Phys. Rev. Lett.* **100**, 040401 (2008).
- [24] J.-Q. Liang, J.-L. Liu, W.-D. Li, and Z.-J. Li, Atom-pair tunneling and quantum phase transition in the strong-interaction regime, *Phys. Rev. A* **79**, 033617 (2009).
- [25] D. Rubeni, J. Links, P. S. Isaac, and A. Foerster, Two-site Bose-Hubbard model with nonlinear tunneling: Classical and quantum analysis, *Phys. Rev. A* **95**, 043607 (2017).
- [26] J. Pietraszewicz, T. Sowiński, M. Brewczyk, J. Zakrzewski, M. Lewenstein, and M. Gajda, Two-component Bose-Hubbard model with higher-angular-momentum states, *Phys. Rev. A* **85**, 053638 (2012).
- [27] M. Alexanian, Scattering of two coherent photons inside a one-dimensional coupled-resonator waveguide, *Phys. Rev. A* **81**, 015805 (2010).
- [28] M. Alexanian, Two-photon exchange between two three-level atoms in separate cavities, *Phys. Rev. A* **83**, 023814 (2011).
- [29] Y. L. Dong, S. Q. Zhu, and W. L. You, Quantum-state transmission in a cavity array via two-photon exchange, *Phys. Rev. A* **85**, 023833 (2012).
- [30] A. Ü. C. Hardal and Ö. E. Müstecaplıoğlu, Transfer of spin squeezing and particle entanglement between atoms and photons in coupled cavities via two-photon exchange, *J. Opt. Soc. Am. B* **29**, 1822 (2012).
- [31] A. Ü. C. Hardal and Ö. E. Müstecaplıoğlu, Spin squeezing, entanglement, and coherence in two driven, dissipative, nonlinear cavities coupled with single- and two-photon exchange, *J. Opt. Soc. Am. B* **31**, 1402 (2014).
- [32] G. Taian, A. V. Dodonov, Two-photon exchange interaction from Tavis-Cummings Hamiltonian under parametric modulation, arXiv:1703.00836 [quant-ph].
- [33] H. Wang, S. Masis, R. Levi, O. Shtempluk, and E. Buks, Off resonance coupling between a cavity mode and an ensemble of driven spins, arXiv:1703.03311 [quant-ph].
- [34] M. Aspelmeyer, T. J. Kippenberg, and F. Marquardt, Cavity Optomechanics, *Rev. Mod. Phys.* **86**, 1391 (2014).
- [35] M. Ludwig, K. Hammerer, and F. Marquardt, Entanglement of mechanical oscillators coupled to a nonequilibrium environment, *Phys. Rev. A* **82**, 012333 (2010).
- [36] H. Seok, L. F. Buchmann, S. Singh, and P. Meystre, Optically mediated nonlinear quantum optomechanics, *Phys. Rev. A* **86**, 063829 (2012).
- [37] H. Seok, L. F. Buchmann, E. M. Wright, and P. Meystre, Multimode strong-coupling quantum optomechanics, *Phys. Rev. A* **88**, 063850 (2013).
- [38] L. F. Buchmann and D. M. Stamper-Kurn, Nondegenerate multimode optomechanics, *Phys. Rev. A* **92**, 013851 (2015).
- [39] X. W. Xu, Y. J. Zhao, and Y. X. Liu, Entangled-state engineering of vibrational modes in a multimembrane optomechanical system, *Phys. Rev. A* **88**, 022325 (2013).
- [40] J. D. Thompson, B. M. Zwickl, A. M. Jayich, F. Marquardt, S. M. Girvin, and J. G. E. Harris, Strong dispersive coupling of a high-finesse cavity to a micromechanical membrane, *Nature (London)* **452**, 72 (2008).
- [41] M. Eichenfield, R. Camacho, J. Chan, K. J. Vahala, and O. Painter, Optomechanical crystals, *Nature (London)* **459**, 550 (2009).
- [42] S. M. Meenehan, J. D. Cohen, G. S. MacCabe, F. Marsili, M. D. Shaw, and O. Painter, Pulsed Excitation Dynamics of an Optomechanical Crystal Resonator near Its Quantum Ground State of Motion, *Phys. Rev. X* **5**, 041002 (2015).
- [43] T. K. Paraíso, M. Kalaei, L. Zang, H. Pfeifer, F. Marquardt, and O. Painter, Position-Squared Coupling in a Tunable Photonic Crystal Optomechanical Cavity, *Phys. Rev. X* **5**, 041024 (2015).
- [44] K. Jähne, C. Genes, K. Hammerer, M. Wallquist, E. S. Polzik, and P. Zoller, Cavity-assisted squeezing of a mechanical oscillator, *Phys. Rev. A* **79**, 063819 (2009).
- [45] X. W. Xu, Y. X. Liu, C. P. Sun, and Y. Li, Mechanical PT symmetry in coupled optomechanical systems, *Phys. Rev. A* **92**, 013852 (2015).
- [46] H. Okamoto, A. Gourgout, C. Y. Chang, K. Onomitsu, I. Mahboob, E. Y. Chang, and H. Yamaguchi, Coherent phonon manipulation in coupled mechanical resonators, *Nature Phys.* **9**, 480 (2013).
- [47] P. Huang, P. F. Wang, J. W. Zhou, Z. X. Wang, C. Y. Ju, Z. M. Wang, Y. Shen, C. K. Duan, and J. F. Du, Demonstration of Motion Transduction Based on Parametrically Coupled Mechanical Resonators, *Phys. Rev. Lett.* **110**, 227202 (2013).
- [48] D. Vitali, S. Gigan, A. Ferreira, H. R. Böhm, P. Tombesi, A. Guerreiro, V. Vedral, A. Zeilinger, and M. Aspelmeyer, Optomechanical Entanglement between a Movable Mirror and a Cavity Field, *Phys. Rev. Lett.* **98**, 030405 (2007).
- [49] T. A. Palomaki, J. W. Harlow, J. D. Teufel, R. W. Simmonds, and K. W. Lehnert, Coherent state transfer between itinerant microwave fields and a mechanical oscillator, *Nature (London)* **495**, 210 (2013).
- [50] J. D. Cohen, S. M. Meenehan, G. S. MacCabe, S. Groblacher, A. H. Safavi-Naeini, F. Marsili, M. D. Shaw, and O. Painter, Phonon counting and intensity interferometry of a nanomechanical resonator, *Nature (London)* **520**, 522 (2015).